*Research Article*

MOLECULAR PAIN

Molecular Pain
Volume 12: 1–15

DOI: 10.1177/1744806916656189
mpx.sagepub.com
SAGE

# Intact subepidermal nerve fibers mediate mechanical hypersensitivity via the activation of protein kinase C gamma in spared nerve injury

**Miau-Hwa Ko, PhD[1], Ming-Ling Yang, PhD[2,3], Su-Chung Youn, PhD[2,3], Chyn-Tair Lan, PhD[2,3] and To-Jung Tseng, PhD[2,3]**

## Abstract

**Background:** Spared nerve injury is an important neuropathic pain model for investigating the role of intact primary afferents in the skin on pain hypersensitivity. However, potential cellular mechanisms remain poorly understood. In phosphoinositide-3 kinase pathway, pyruvate dehydrogenase kinase 1 (PDK1) participates in the regulation of neuronal plasticity for central sensitization. The downstream cascades of PDK1 include: (1) protein kinase C gamma (PKCγ) controls the trafficking and phosphorylation of ionotropic glutamate receptor; (2) protein kinase B (Akt)/the mammalian target of rapamycin (mTOR) signaling is responsible for local protein synthesis. Under these statements, we therefore hypothesized that an increase of PKCγ activation and mTOR-dependent PKCγ synthesis in intact primary afferents after SNI might contribute to pain hypersensitivity.

**Results:** The variants of spared nerve injury were performed in Sprague-Dawley rats by transecting any two of the three branches of the sciatic nerve, leaving only one branch intact. Following SNIt (spared tibial branch), mechanical hyperalgesia and mechanical allodynia, but not thermal hyperalgesia, were significantly induced. In the first footpad, normal epidermal innervations were verified by the protein gene product 9.5 (PGP9.5)- and growth-associated protein 43 (GAP43)-immunoreactive (IR) intraepidermal nerve fibers (IENFs) densities. Furthermore, the rapid increases of phospho-PKCγ- and phospho-mTOR-IR subepidermal nerve fibers (SENFs) areas were distinct gathered from the results of PGP9.5-, GAP43-, and neurofilament 200 (NF200)-IR SENFs areas. The efficacy of PKC inhibitor (GF 109203X) or mTOR complex 1 inhibitor (rapamycin) for attenuating mechanical hyperalgesia and mechanical allodynia by intraplantar injection was dose-dependent.

**Conclusions:** From results obtained in this study, we strongly recommend that the intact SENFs persistently increase PKCγ activation and mTOR-dependent PKCγ synthesis participate in the initiation and maintenance of mechanical hypersensitivity in spared nerve injury, which represents as a novel insight into the therapeutic strategy of pain in the periphery.

## Keywords

Spared nerve injury, mechanical hypersensitivity, intraepidermal nerve fibers, subepidermal nerve fibers, protein kinase C gamma, the mammalian target of rapamycin, GF 109203X, rapamycin

Date received: 12 March 2016; revised: 17 May 2016; accepted: 23 May 2016

[1]Department of Anatomy, College of Medicine, China Medical University, Taichung, Taiwan
[2]Department of Anatomy, School of Medicine, Chung Shan Medical University, Taichung, Taiwan
[3]Department of Medical Education, Chung Shan Medical University Hospital, Taichung, Taiwan

**Corresponding author:**
Chyn-Tair Lan, Department of Anatomy, School of Medicine, Chung Shan Medical University, No. 110, Jian-Guo N. R., Sec. 1, Taichung 40201, Taiwan.
Email: ctlan@csmu.edu.tw
To-Jung Tseng, Department of Anatomy, School of Medicine, Chung Shan Medical University, No. 110, Jian-Guo N. R., Sec. 1, Taichung 40201, Taiwan.
Email: tjtseng@csmu.edu.tw

## Background

Clinically, patients suffering from sciatic nerve damages show the obvious symptoms of hyperalgesia, allodynia, and spontaneous pain. Several neuropathic pain models, including partial sciatic nerve ligation, chronic constriction injury (CCI), and spared nerve injury (SNI), have been established in animals.[1–3] In SNI, standard surgical

procedure is performed on the sciatic nerve with complete transection of the tibial and common peroneal branches while leaving the sural branch intact.[3] Pain hypersensitivity after SNI is usually linked to the occurrences of thermal hyperalgesia, cold allodynia, mechanical hyperalgesia, and mechanical allodynia.[4,5] Several manipulations, such as physiological recordings, morphological distributions, and drug administrations, have been used to evaluate pain-related analysis in SNI.[6–8]

Primary afferents in the epidermis, known as intraepidermal nerve fibers (IENFs), have been used to evaluate the integrity of C and Aδ fibers by immunohistochemistry. Protein gene product 9.5 (PGP9.5) is commonly applied to illustrate the degree of IENFs degeneration and regeneration in inflammatory and neuropathic pain models.[9–11] Furthermore, an increased capacity of IENFs regeneration is elucidated by a result of growth-associated protein 43 (GAP43) expressions following nerve decompression in CCI.[12] Neurofilament 200 (NF200) is expressed in the medium- and large-sized neurons of the dorsal root ganglion, which are restricted to recognize myelinated Aδ and Aβ fibers.[13] We have recently demonstrated a decrease of subepidermal nerve fibers (SENFs) after CCI by calculating NF200 and calcitonin gene-related peptide (CGRP) expressions in the dermis.[14]

Protein kinase C gamma (PKCγ), one of the conventional PKC isoforms, is widely distributed throughout the central nervous system, including trigeminal spinal nucleus, gracile nucleus, and dorsal horn neurons.[15,16] In chronic pain state, a persistent increase of PKCγ maintains neuronal plasticity in the dorsal horn following a cellular mechanism of ''pain memory,'' which parallels studies from long-term potentiation in the hippocampus.[17–19] In recent times, PKCγ activated by 5-HT2B or EphB receptor resulting in the phosphorylation of N-Methyl-D-aspartate (NMDA) receptors mediates the onset of thermal hyperalgesia and mechanical allodynia.[20,21] Growing evidences suggest that a selective PKC inhibitor, GF 109203X, has been efficiently used to attenuate these pain hypersensitivity by intrathecal injection.[20,22] Interestingly, SNI-induced mechanical allodynia is obviously reduced in PKCγ knockout mice, but enhanced in PKCα knockout mice.[23,24]

The mammalian target of rapamycin (mTOR) is generally found within neurons in the dorsal root ganglion and dorsal horn.[25] mTOR binds Raptor to form mTOR complex 1, which modulates eukaryotic initiation factor 4E-binding protein 1 (4E-BP1) and p70 ribosomal S6 protein kinase 1 (S6K1) to promote local protein synthesis.[25,26] In neuropathic and inflammatory pain models, the activation of mTOR and S6K1 enhances neuronal plasticity in the dorsal horn leading to pain hypersensitivity.[27,28] Additionally, intact myelinated A fibers of the skin and spinal rootlets following SNI increase the activity of 4E-BP1 and S6K1, which are also in response to pain hypersensitivity.[29,30] Rapamycin and temsirolimus, the inhibitors of mTOR complex 1, are successfully applied to intrathecal or intraplantar injection.[28–31] A possible mechanism has been showed that tyrosine kinase B (TrkB) receptors regulated by brain-derived neurotrophic factors (BDNF) increase the local PKCλ and protein kinase M zeta (PKMζ) synthesis via the mTOR signaling in dorsal horn.[32,33]

Based on the above-mentioned evidences, the present study was set out to (1) compare the temporal changes of thermal hyperalgesia, mechanical hyperalgesia, and mechanical allodynia in Sprague-Dawley rats after the variants of SNI; (2) interpret the possible changes of epidermal innervation and dermal distribution in the first footpad by using the immunohistochemistry; and (3) clarify the role of PKCγ based on the results of morphological observation and therapeutic intervention.

## Methods and materials

### Experimental animals

Adult male Sprague-Dawley rats, weighing 200–250 g, were housed in plastic cages with soft sawdust as bedding to avoid mechanical damage to the footpad. The cages were kept in a temperature and humidity-controlled room with a 12-h light/dark cycle. Food and water were available ad libitum. All procedures were conducted in accordance with the ethical guidelines set up by the International Association for the Study of Pain (IASP) on the use of laboratory animals in experimental research, and the study protocol was approved by the Animal Committee of China Medical University, College of Medicine, Taichung, Taiwan.[34,35]

### Surgical procedures

The variants of SNI were performed on Sprague-Dawley rats following the established procedures as previously descripted[5] (Figure 1). In brief, under pentobarbital anesthesia (60 mg/kg, i.p.), the right sciatic nerve was exposed at the mid-thigh level by freeing the adhering fascia between gluteus and biceps femoris muscles. Ligatures of 6–0 silk (Ethicon, Johnson, and Johnson Intl, Brussels, Belgium) were tightly tied around any two of the three branches of the sciatic nerve and transected distal to the ligations (Figure 1(a)). The standard surgical procedure for SNI was defined as SNIs in this study.[3] Thus, SNIt (spared tibial branch) and SNIcp (spared common peroneal branch) were individually preserved with their own branch intact. In addition, complete nerve transection defined as SNT was separately ligated and transected below the trifurcation of sciatic nerve.[36] For rats in the operation control group,

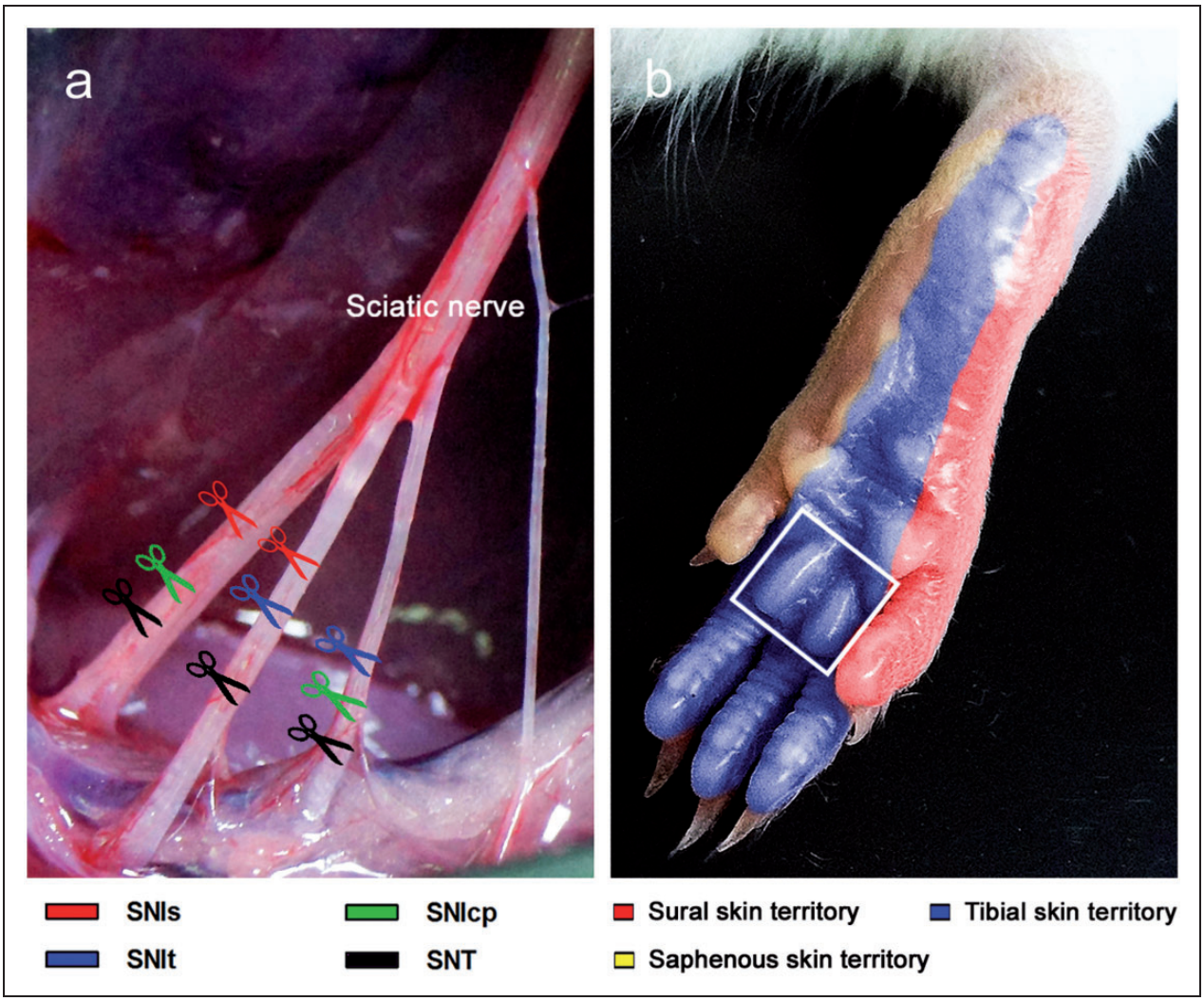


**Figure 1.** Manipulations for establishing the variants of SNI and SNT. (a) The variants of SNI were performed in Sprague-Dawley rats by transecting any two of the three branches of the sciatic nerve, leaving any one branch intact. Therefore, three experimental groups (SNIs, SNIt, and SNIcp) were established. In the group of SNT, all the branches were transected separately, while all the branches were exposed without transection in operation control group, known as Sham. (b) Lateral (sural skin territory) and central sides (tibial skin territory) innervated by the individual branches of the sciatic nerve are represented as appropriate receptive fields in the foot sole. Additionally, the medial side of the foot sole was innervated by the branch of the femoral nerve (saphenous skin territory). Hollow square indicates the region of the first footpad, which was used for evaluating the behavioral assessments and cutaneous innervations in the present study.

designated as Sham, the sciatic nerve was exposed without ligation and transection.

### *Study design*

A total of five experimental groups (SNIs, SNIt, SNIcp, SNT, and Sham) ($n = 15$ for each group) were arranged to examine the hypothesis of this study. Behavioral hypersensitivity, including thermal hyperalgesia, mechanical hyperalgesia, and mechanical allodynia, was assessed by the administration of stimuli on the first footpad, mainly the tibial skin territory (Figure 1(b)). Behavioral assessments were evaluated at the following time points: postoperative week 0 (POW0) (designated as the pretest baseline data), POW1, POW2, and POW4. Then, all rats were sacrificed periodically at POW1, POW2, and POW4 ($n = 5$ per time point for each group). The major rationale for the choice of such an order was to observe the possible influence of collateral sprouting on cutaneous innervations.

### *Thermal Hyperalgesia*

Thermal hyperalgesia was estimated by measuring the withdrawal latency upon stimulation of radiant heat using a Hargreaves-type analgesiometer (Ugo Basile,

Comerio-Varese, Italy). The rats were individually placed in one of the three separate Plexiglas containers (22 $\times$ 17 $\times$ 14 $cm^3$) located on an elevated floor of a clear glass plate (3 mm thick) and were allowed 30 min to habituate themselves to this apparatus. A radiant heat source (a halogen projector lamp, 50 W, 8 V) was placed directly beneath the first footpad.[37] Withdrawal latency was automatically measured as the time elapsed from the onset of stimulation to the removal of the hindpaw by the rat. A maximum time of 20 s for thermal stimulation was imposed to avoid possible tissue damage. The readings were recorded to the nearest 0.1 s, and the average of five consecutive measurements was taken as the thermal threshold.

### Mechanical hyperalgesia

A pin-prick test was performed using a safety pin to decide a withdrawal response period, defined as the pin-prick duration.[38] The rats were individually placed in one of the three separate Plexiglas containers on a wire mesh floor and allowed to acclimate for 10 min. The tip of a safety pin was used to prick the first footpad at a strength enough to produce a withdrawal response but did not penetrate. The pin-prick duration was recorded using a stopwatch as the time elapsed from the beginning of hindpaw removal to placing it back on the wire mesh floor. A minimum duration of 0.5 s was assigned preoperatively. A cut-off time of 15 s for safety pin stimulation was set to avoid possible tissue damage. The readings were recorded to the nearest 0.01 s, and the average of five consecutive measurements was taken as the pin-prick duration.

### Mechanical allodynia

Mechanical threshold was determined by measuring a withdrawal response according to an up-and-down method using a series of calibrated von Frey monofilaments (Senselab aesthesiometer, Somedic Sales AB, Stockholm, Sweden).[10] The rats were individually placed in one of the three separate Plexiglas containers on a wire mesh floor and allowed to acclimate for 10 min. The examiner touched the first footpad with a monofilament for 1 s until the bending angle reached 45° and a brisk withdrawal or paw flinching was noted, which was considered as a positive response. Mechanical threshold was defined as the minimum force (g) applied by a von Frey monofilament which initiated a positive withdrawal response of the hindpaw.

### Immunohistochemistry

At the end of all experiments, the rats were deeply anesthetized using pentobarbital (100 mg/kg, i.p.) and sacrificed by intracardiac perfusion of 4% paraformaldehyde in 0.1 M phosphate buffer (PB) at pH 7.4. After perfusion, the footpads were removed and further immersed in fixative for additional 6 h before shifted to 0.1 M PB for storage. Prior to sectioning, samples were rinsed thoroughly, cryoprotected with 30% sucrose in 0.1 M PB overnight, and then cut at a plane perpendicular to the epidermis in a thickness of 30 μm per section with a sliding microtome (HM440E; Microm, Walldorf, Germany), labeled sequentially, and stored at −20°C.

To ensure adequate and systematic sampling, every sixth section was chosen, resulting in a total of four frozen sections from each footpad. The sections were treated with 0.5% Triton X-100 in 0.5 M Tris buffer (Tris), pH 7.6, for 30 min and processed for immunohistochemical staining. Briefly, the sections were quenched with 1% $H_2O_2$ in methanol, blocked with 5% normal goat serum in 0.5% nonfat dry milk/Tris, and then incubated with the following primary antisera overnight, respectively: (1) rabbit polyclonal PGP9.5 (1: 1000, UltraClone, Isle of Wight, UK); (2) rabbit polyclonal GAP43 (1:1000, Millipore, Billerica, MA); (3) rabbit polyclonal NF200 (1:1000, Sigma Chemicals, St. Louis, MO); (4) rabbit monoclonal phospho-PKCγ (1:100, Epitomics, Burlingame, CA); and (5) rabbit monoclonal phospho-mTOR (1:1000, Cell Signaling Technology, Beverly, MA). After rinsing in Tris, the sections were incubated with biotinylated goat anti-rabbit IgG for 1 h followed by avidin-biotin complex horseradish peroxidase reagent (Vector Laboratories, Burlingame, CA) for another hour. The reaction products were demonstrated with 3,3′-diaminobenzidine (DAB, Sigma Chemicals, St. Louis, MO).

### IENFs Density

Epidermal innervation was quantified following a well-known protocol in a coded fashion.[10] Immunoreactivities of PGP9.5 and GAP43 in the epidermis were assessed at a magnification of 40 $\times$ by an Olympus BX40 microscope (Olympus, Tokyo, Japan). Each individual nerve fiber with branching points inside the epidermis was counted as one. For nerve fibers with branching points in the dermis, each branch was counted separately. Epidermal length of 2.5 mm along the upper margin of stratum corneum was measured with a Sigma Scan (SPSS, Chicago, IL). IENFs density was derived and expressed as the number of fibers per centimeter of epidermal length. Every fourth section was quantified, and the mean derived from these four sections was defined as the IENFs density of that rat.

### SENFs area

The standard procedure for measuring SENFs area was modified from a protocol published in our previous study.[14] In brief, high-definition monochrome images were photographed under an Olympus microscope (BH2; Olympus, Tokyo, Japan) with a digital camera

at a magnification of 10×. Dermal area was therefore defined as an area within a width of 2.5 mm in epidermal length and at a depth of 200 μm below the dermal–epidermal junction. All the areas of interest were edited by Magic Wand Tool (tolerance: 100) to eliminate noises from background staining (collagen fibers of the dermis) and calculated with Adobe Photoshop Elements 9.0 (Adobe Systems, San Jose, CA, USA). The area of interest was measured in pixels then transformed to $\mu m^2$ according to the relationships between pixel size and magnification. Every fourth section was quantified and the mean of these four SENFs areas was defined as the SENFs area of that rat.

### *Merkel cell density*

The protocol for the quantification of Merkel cell distribution was modified from a method published previously.[39] Immunoreactivity of PGP9.5 in the epidermis was assessed at a magnification of 40 × with an Olympus BX40 microscope. Each individual Merkel cell with an ovoid profile inside the epidermis was counted as one. Epidermal length of 2.5 mm along the upper margin of stratum corneum was measured using a Sigma Scan (SPSS, Chicago, IL), and Merkel cell density was derived and expressed as the number of cells per centimeter of epidermal length. Every fourth section was quantified and the mean derived from these four sections was defined as the Merkel cell density of that rat.

### *Drug administration*

A vehicle solution was prepared with 10% dimethyl sulfoxide (DMSO, Sigma, St. Louis, MO) and 80% saline. GF 109203X (MW = 412.49), a selective PKC inhibitor, was obtained from Selleckchem (Houston, TX) and added to vehicle to set up two different final concentrations of 2.5 mM and 0.5 mM, respectively.[40] Rapamycin (MW = 914.19), a mTOR complex 1 inhibitor, was purchased from Cell Signaling Technology (Danvers, MA), and the final concentrations of 500 mM and 250 mM in vehicle solution were set up.[30] Pharmacological agents were administered through intraplantar injection by an established protocol for the purpose of reducing inflammatory responses.[41] Briefly, under ether anesthesia, a 26-gauge needle connected to a 10 μL Hamilton syringe (model: 701; Hamilton Company, Reno, NV, USA) was subdermally inserted into the plantar aspect of the surgical side. A volume of 10 μL of the pharmacological agents per rat was slowly injected for about 30 s.

### *Assessment of drug delivery*

In this evaluation, we first established the baseline values of behavioral hypersensitivity at one week after SNIt and Sham, defined as the PIH0. According to the concentrations of GF 109203X (2.5 mM, 0.5 mM, and vehicle) and rapamycin (500 mM, 250 mM, and vehicle) in both treatments, the rats after SNIt were randomly separated into three groups ($n = 5$ for each group per treatment). In addition, the rats after Sham were treated only with the maximum concentration ($n = 5$ per treatment). After intraplantar injection, all rats were assessed at 2, 4, 6, and 24 h (PIH2, PIH4, PIH6, and PIH24), respectively, to evaluate behavioral hypersensitivity. The rationale for the choice of such an order was in performing the least stressful measurement to first minimize the influence of the next measurement on the result and to avoid tissue damage. The sequence of behavioral assessments was kept the same until the end of experiments for all the rats.

### *Statistical analysis*

Examiners were blinded to the grouping information when performing all the laboratory procedures of measurement and quantification. Behavioral assessments and the quantification of IENFs density, SENFs area, and Merkel cell density were represented as mean ± standard deviation (SD) using GraphPad Prism (GraphPad, San Diego, CA, USA). Data obtained from withdrawal responses and morphological examinations at each corresponding time point were analyzed by Student's $t$ test. For the data that did not follow a Gaussian distribution, a nonparametric Mann–Whitney $U$ test was conducted. A statistically significant difference was considered when $p < 0.05$. Temporal changes of behavioral assessments were analyzed by two-way repeated measures analysis of variance (ANOVA) following a Bonferroni's post hoc test when $p < 0.05$ was obtained. To analyze within-group behavioral differences after drug administration, one-way repeated measures ANOVA was performed following the Dunnett's multiple comparison tests when $p < 0.05$ was obtained.

## Results

### *Surgical designs and correspondent skin territory*

The variants of SNI were performed on Sprague-Dawley rats following established procedures as previously descripted[5] (Figure 1(a)). The standard surgical procedure for SNI was defined as SNIs (spared sural branch) in this study.[3] Hence, own intact branch in SNIt (spared tibial branch) and SNIcp (spared common peroneal branch) were individually preserved. Moreover, complete nerve transection defined as SNT was separately ligated and transected below the trifurcation of sciatic nerve.[36] While in the operation control group, the sciatic nerve exposed without ligation and transection was designated as Sham. Behavioral assessments, including thermal

hyperalgesia, mechanical hyperalgesia, and mechanical allodynia, were measured by administration of stimuli on the first footpad, which is mainly the tibial skin territory (Figure 1(b)).

### *Behavioral assessment following the variants of SNI and SNT*

The thresholds of withdrawal responses on the first footpad after the variants of SNI, SNT, and Sham were examined by radiant heat, pin-prick, and von Frey monofilament (Figure 2). Between SNIt and Sham, there was no significant difference in withdrawal latency throughout POW1 to POW4 (Figure 2(a)). In contrast, the apparent increases of withdrawal latency were shown following SNIs, SNIcp, and SNT, and were defined as thermal hypoalgesia. The increases of pin-prick duration were obviously exhibited after SNIt throughout the entire experimental period (Figure 2(b)), while mechanical hypoalgesia was confirmed by the noticeable decreases of pin-prick duration following the other SNI and SNT. After SNIt, significant reductions in mechanical threshold were observed from POW1 to POW4 (Figure 2(c)). However, mechanical thresholds were considerably increased following SNIs, SNIcp, and SNT.

### *Changes in epidermal innervation after the variants of SNI and SNT*

After the variants of SNI, SNT, and Sham, the morphological patterns of immunoreactive (IR) IENFs at POW1 were used to demonstrate epidermal innervations in the first footpad (Figure 3). After SNIt, a lot of PGP9.5-IR IENFs originated from subepidermal nerve plexus penetrated through epidermal–dermal junction and ascended perpendicularly with typical varicosities in the epidermis were observed (Figure 3(a)). The entire loss of PGP9.5-IR IENFs began from POW1 following SNIs, SNIcp, and SNT indicating the complete IENFs degeneration (Figure 3(c)). PGP9.5-IR IENFs after Sham showed a similar pattern like that after SNIt (Figure 3(e)). Because of the complete epidermal denervation following SNIs, SNIcp, and SNT, we only described the temporal changes of PGP9.5-IR IENFs density after SNIt and Sham here (Figure 3(g)). The results demonstrated that PGP9.5-IR IENFs densities after SNIt were equal to those measured after Sham from POW1 to POW4. After SNIt, GAP43-IR IENFs were initiated from subepidermal nerve plexus and rose vertically with tiny varicosities in the epidermis (Figure 3(b)). At POW1 following SNIs, SNIcp, and SNT, complete epidermal denervation was also illustrated by a complete loss of GAP43-IR IENFs (Figure 3(d)). These GAP43-IR IENFs after Sham represented a normal epidermal innervation, equivalent to that observed after SNIt (Figure 3(f)). All the GAP43-IR IENFs densities were comparable between SNIt and Sham until the end of experiments (Figure 3(h)).

### *Comparisons of dermal distribution between SNIt and Sham*

Dermal distributions of IR SENFs in the first footpad were illustrated by morphological patterns observed following SNIt and Sham at POW1, and temporal changes of IR SENFs were verified by the quantification of IR area (Figure 4). After SNIt, PGP9.5-IR SENFs extended from dermal nerve bundles and formed dense subepidermal nerve plexuses nearby epidermal–dermal junction (Figure 4(a)). A similar distribution of PGP9.5-IR SENFs was found in the dermis after Sham (Figure 4(b)). Comparable PGP9.5-IR SENFs areas from POW1 to POW4 were demonstrated between SNIt and Sham (Figure 4(c)). GAP43-IR SENFs, starting from dermal nerve bundles after SNIt, formed an irregular nerve fiber meshwork close to epidermal–dermal junction (Figure 4(d)). Dermal distributions of GAP43-IR SENFs after Sham were similar to those after SNIt (Figure 4(e)). Moreover, NF200-IR SENFs originated from dermal nerve bundles after SNIt were terminated adjacent to dermal papillae with typical rod-like blunt stumps (Figure 4(g)). A similar distribution of NF200-IR SENFs was observed in the dermis after Sham (Figure 4(h)). No obvious difference in GAP43- and NF200-IR SENFs areas was found after SNIt and Sham until the end of experiments (Figure 4(f) and (i)).

### *Increases of PKC$\gamma$ and mTOR expression in intact SENFs following SNIt*

In the first footpad, we showed the morphological patterns of phospho-PKCγ- and phospho-mTOR-IR SENFs following SNIt and Sham at POW1 (Figure 5). After SNIt, phospho-PKCγ-IR SENFs extended from dermal nerve bundles towards epidermal–dermal junction with elongated fragments (Figure 5(a)). Relatively, phospho-PKCγ-IR SENFs displayed shortened fragments in dermal nerve bundles after Sham (Figure 5(b)). Beginning from POW1 through POW4, significant differences in phospho-PKCγ-IR SENFs areas between SNIt and Sham were exposed (Figure 5(c)). After SNIt, phospho-mTOR-IR SENFs reached out from dermal nerve bundles nearby epidermal–dermal junction with discontinuous fragments (Figure 5(d)). Dotted appearances were mostly shown in phospho-mTOR-IR SENFs after Sham (Figure 5(e)). The increased phospho-mTOR-IR SENFs areas after SNIt were significant comparing to those after Sham until the end of experiments (Figure 5(f)).

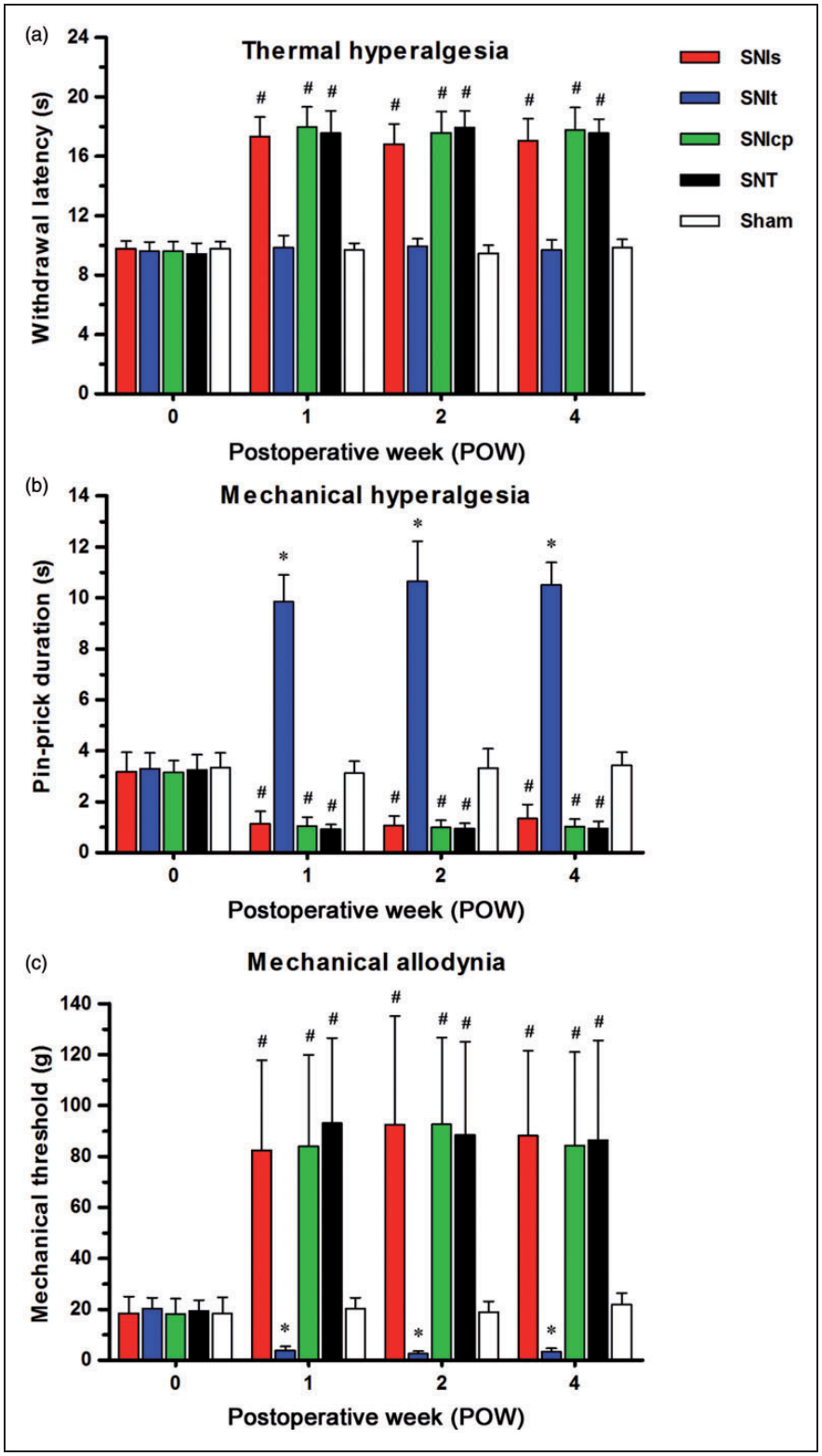


**Figure 2.** Comparisons of pain hypersensitivity following the variants of SNI and SNT. Temporal changes of pain hypersensitivity were showed in (a) thermal hyperalgesia, noxious radiant heat stimulus-evoked thermal threshold was defined as the withdrawal latency (s); (b) mechanical hyperalgesia, safety pin-evoked withdrawal response period was measured as the pin-prick duration (s); and (c) mechanical allodynia, the degree of von Frey monofilament-evoked withdrawal response was expressed as the mechanical threshold (g). Behavioral assessments were represented as mean $\pm$ SD ($n = 5$ at each POW in each group). Student's $t$ test was applied to examine the differences against Sham at each time point. * $p < 0.05$ indicated a significant difference versus Sham (hypersensitivity) and # $p < 0.05$ indicated a significant difference versus Sham (hyposensitivity). Two-way repeated measures ANOVA was also performed following the Bonferroni's post hoc test.

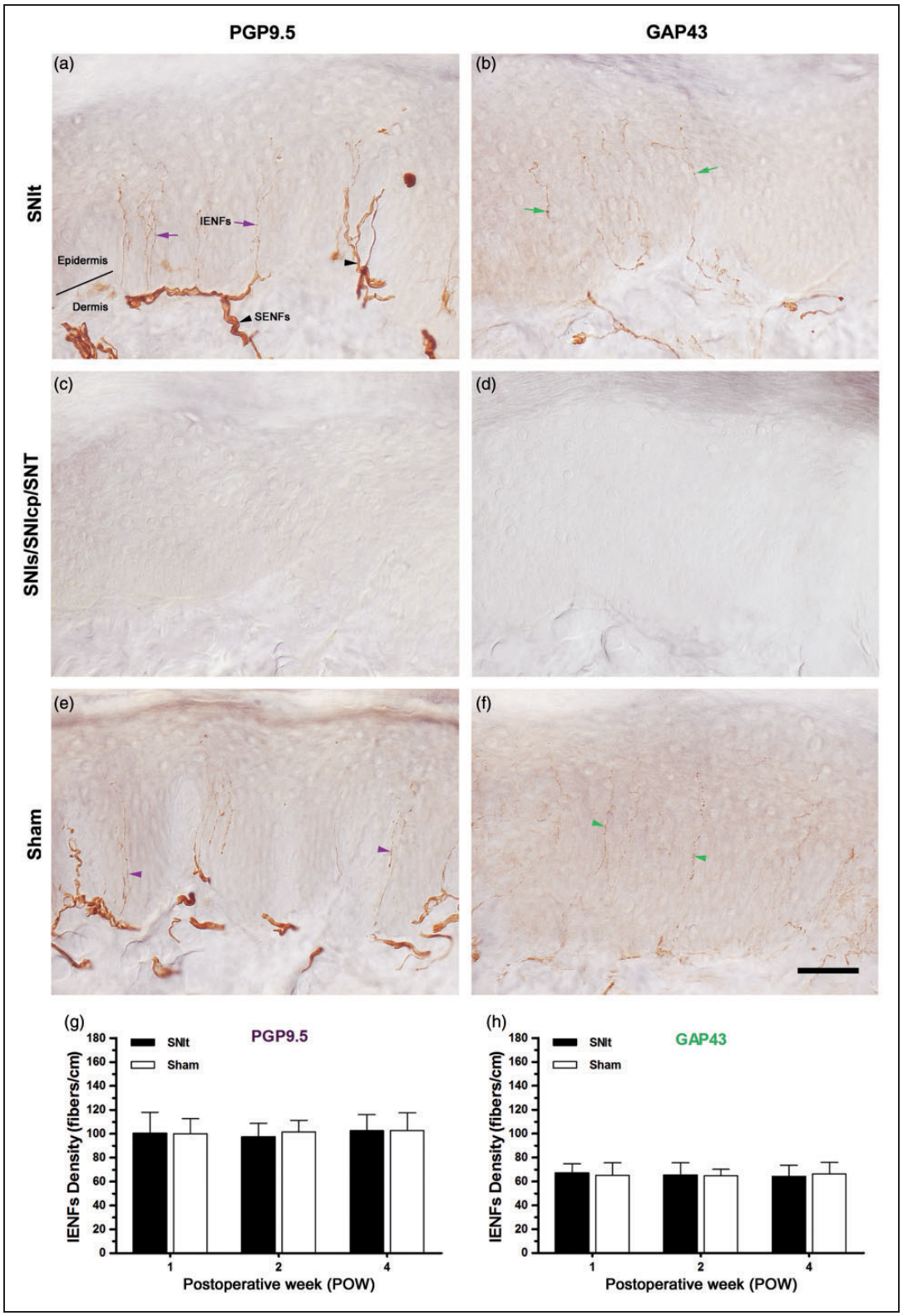


**Figure 3.** Changes in epidermal innervation following the variants of SNI and SNT. At POW1 after (a, b) SNIt, (c, d) SNIs, SNIcp, SNT, and (e, f) Sham, the footpad sections were immunostained with antisera against (a, c, e) PGP9.5 and (b, d, f) GAP43. Epidermal innervations following SNIt and Sham were quantified by the temporal changes of the morphological patterns in (g) PGP9.5 and (h) GAP43 expressions, which were represented as IENFs Density (mean ± SD; $n = 5$ at each POW after SNIt and Sham). Student's $t$ test was applied to examine the differences against the results of Sham at each time point. Two-way repeated measures ANOVA was also performed following the Bonferroni's post hoc test.

IENFs: intraepidermal nerve fibers; SENFs: subepidermal nerve fibers; solid line, epidermal–dermal junction. Scale bar = 50 μm.

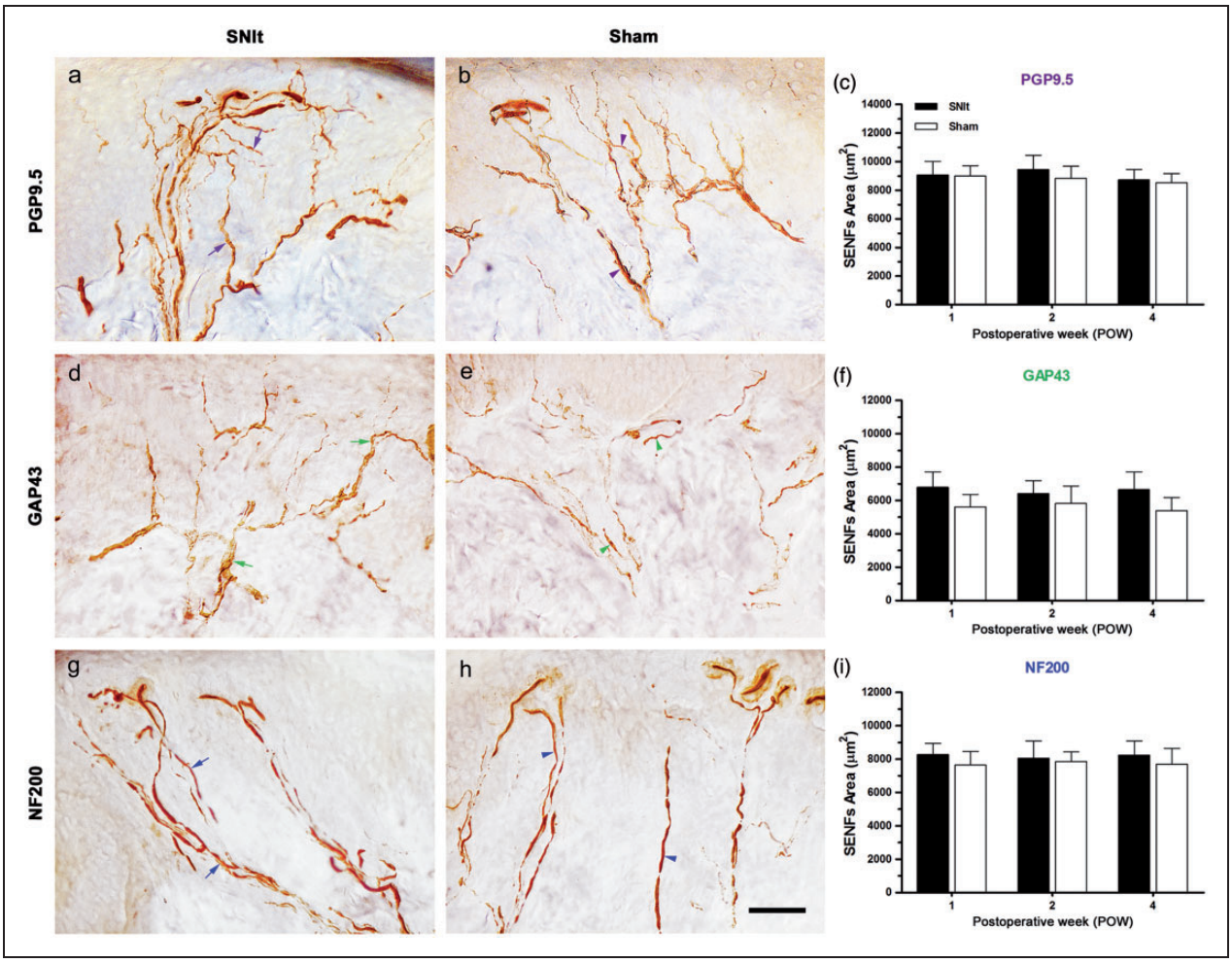


**Figure 4.** Comparisons of dermal distribution between SNIt and Sham. At POW1 after (a, c, e) SNIt and (b, d, f) Sham, the footpad sections were immunostained with antisera against (a, b) PGP9.5, (d, e) GAP43, and (g, h) NF200. Dermal distributions between SNIt and Sham were quantified by the temporal changes of the morphological patterns in (c) PGP9.5, (f) GAP43, and (i) NF200 expressions, which were represented as SENFs Area (mean $\pm$ SD; $n = 5$ at each POW after SNIt and Sham). Student's $t$ test was applied to examine the differences against the results of Sham at each time point. Two-way repeated measures ANOVA was also performed following the Bonferroni's post hoc test. Scale bar = 50 μm.

### *Peripheral effects of drug administration on pain hypersensitivity after SNIt*

By the use of behavioral assessments at POW1, baseline withdrawal responses were measured after SNIt and Sham for the studies on drug administration (Figure 6). After vehicle injection in SNIt, the withdrawal responses did not show any significant difference at each time point as comparing against post injection hour 0 (PIH0) respectively, which were used for evaluating the influence of different drug concentrations. In addition, the maximum drug concentration injected in Sham did not alter normal withdrawal responses during the entire experimental period when comparing against PIH0, respectively.

After GF 109203X injections in SNIt, there was no effect on withdrawal latency observed at all the time points (Figure 6(a)). From PIH2 to PIH6, however, pin-prick durations in SNIt were decreased accordingly with the different doses treated (Figure 6(c)). Besides, both dosages of GF 109203X injected in SNIt rapidly intensified mechanical thresholds till PIH6 (Figure 6(e)). At PIH24, pin-prick durations and mechanical thresholds were bounce back to such as just after vehicle injection in SNIt. Behavioral patterns under the treatments of rapamycin injection in SNIt were similar to those following GF 109203X injections (Figure 6(b), (d), (f)). It should be noted that pin-prick durations and mechanical thresholds in SNIt still showed significant differences at PIH24 between rapamycin and vehicle injections.

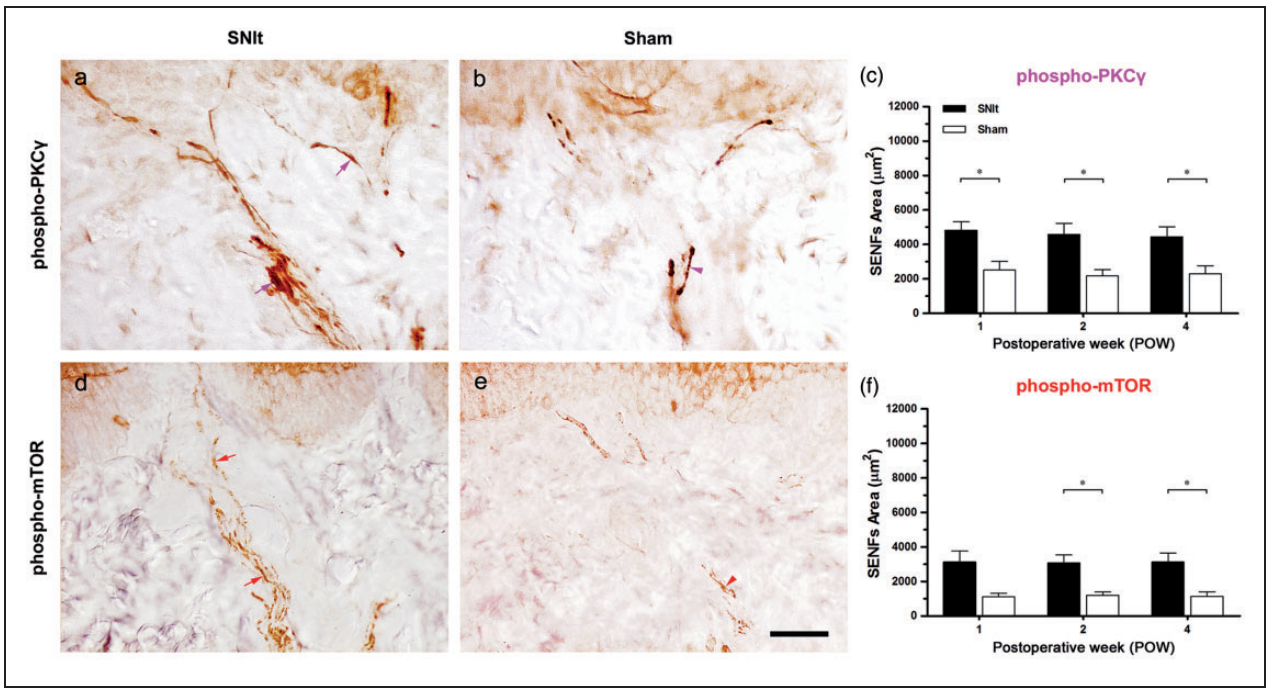


**Figure 5.** Increases of PKCγ and mTOR expression in intact SENFs following SNIt. At POW1 after (a, d) SNIt and (b, e) Sham, the footpad sections were immunostained with antisera against (a, b) phospho-PKCγ and (d, e) phospho-mTOR. Dermal distributions between SNIt and Sham were quantified by the temporal changes of the morphological patterns in (c) phospho-PKCγ and (f) phospho-mTOR, which were represented as SENFs Area (mean ± SD; $n = 5$ at each POW after SNIt and Sham). Student's $t$ test was applied to examine the differences against the results of Sham at each time point. Two-way repeated measures ANOVA was also performed following the Bonferroni's post hoc test. Scale bar = 50 μm.

### *Distributions of Merkel cell in the epidermis following the variants of SNI and SNT*

Changes of PGP9.5-IR Merkel cells observed in the epidermis were shown at POW1 after the variants of SNI, SNT, and Sham (Figure 7). Following SNIt, numerous PGP9.5-IR Merkel cells having an ovoid profile clustered mostly in the stratum basale of the epidermis (Figure 7(a)). Less PGP9.5-IR Merkel cells were found after SNIs, SNIcp, and SNT, which were different from those after Sham (Figure 7(b) and (c)). Quantification following SNIt showed the significant increases in PGP9.5-IR Merkel cell density from POW1 to POW4 when comparing with Sham (Figure 7(d)). In contrast, there were obvious decreases in Merkel cell density after SNIs, SNIcp, and SNT until the end of experiments.

## Discussion

The present findings provide several novel insights into the behaviors, morphology, and pain mechanisms of SNI in the periphery. First, we compared the temporal changes of pain hypersensitivity and related them to cutaneous innervation in the variants of SNI and SNT. Our results showed that the rats after SNIt significantly developed mechanical hyperalgesia and mechanical allodynia, but not thermal hyperalgesia. Based on the integrity of intact IENFs and SENFs in the first footpad after SNIt, the possibility of nerve terminal sprouting in the skin was excluded. Second, we focused on the potential mechanisms of SNIt-induced pain hypersensitivity in intact SENFs. Our results showed that the increases of phospho-PKCγ- and phospho-mTOR-IR expressions were observed in intact SENFs. GF 109203X or rapamycin administrations illustrating the dose-dependent inhibitions to mechanical hyperalgesia and mechanical allodynia via intraplantar injections. These findings verified and strengthened our preliminary assumption that SNI induced an increase of PKCγ activation and mTOR-dependent PKCγ synthesis in intact SENFs, which played an essential role in the initiation and maintenance of mechanical hypersensitivity.

### *Behavioral assessments after the variants of SNI*

SNI, one of the neuropathic pain models, established based on facts gathered from partial sciatic nerve injury is used for evaluating pain hypersensitivity.[3] Therefore, thermal hyperalgesia, cold allodynia,

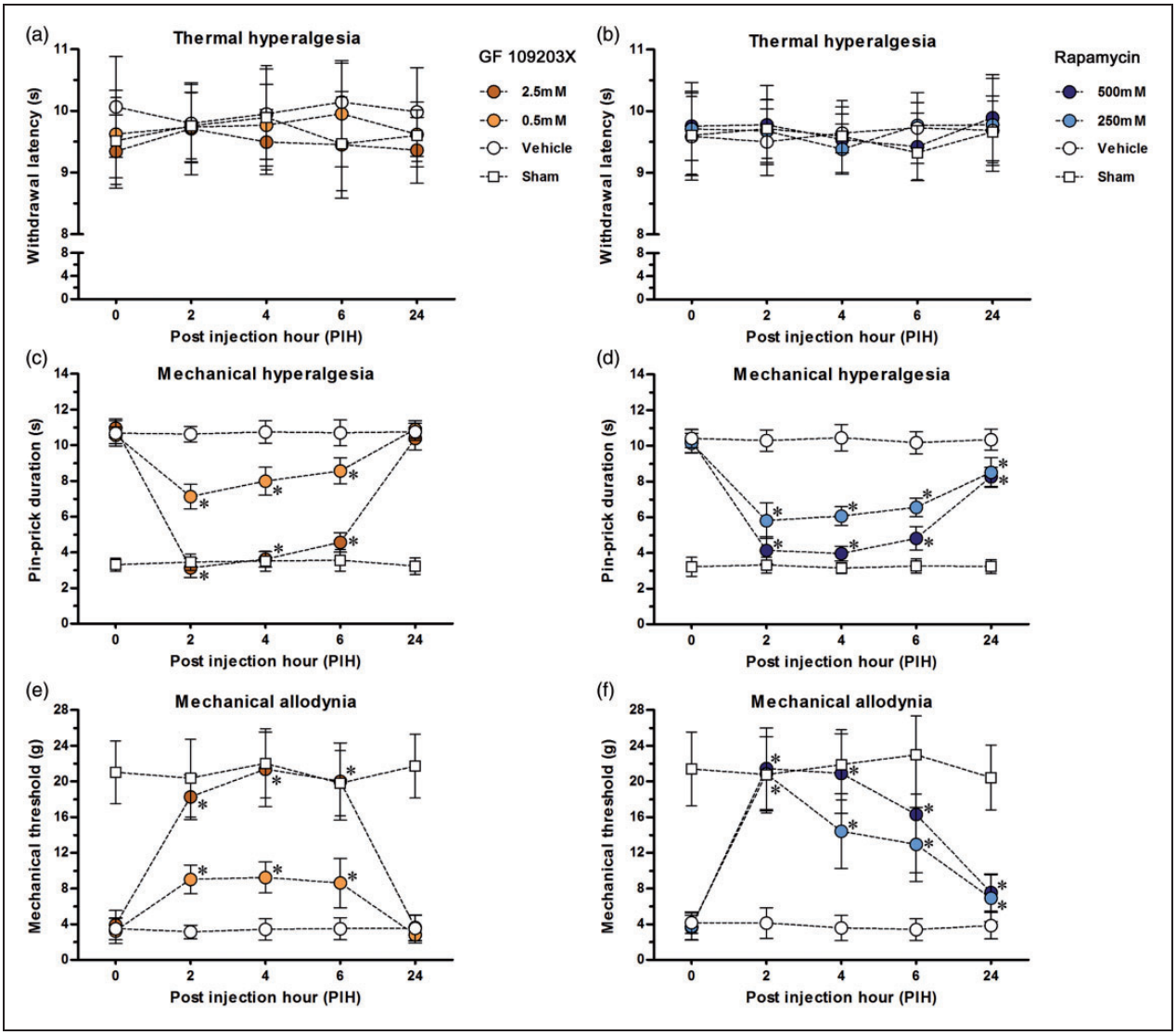


**Figure 6.** Local effects of inhibitors on SNIt-induced mechanical hypersensitivity. (a, c, e) PKC inhibitor (GF 109203X) and (b, d, f) mTOR complex 1 inhibitor (rapamycin) were used in the rats after SNIt and Sham by intraplantar injections for the behavioral assessments of (a, b) thermal hyperalgesia, (c, d) mechanical hyperalgesia, and (e, f) mechanical allodynia. The withdrawal responses in surgical side were represented as mean ± SD in withdrawal latency, pin-prick duration, and mechanical threshold following each PIH. Based on the concentrations of inhibitors, the rats after SNIt were separated into three groups ($n = 5$ for each group) for each treatment. The maximum concentration was used in the rats after Sham ($n = 5$). Student's $t$ test was applied to examine the differences against vehicle injections after SNIt at each time point. * $p < 0.05$ indicated a significant difference. One-way repeated measures ANOVA was also used to analyze within-group differences following the Dunnett's multiple comparison tests.

mechanical hyperalgesia, and mechanical allodynia have been entirely measured.[3–5] In addition, the variants of SNI are further set up to comparing these related pain hypersensitivity.[6,7] In this study, our results showed that the rats after SNIt significantly developed mechanical hyperalgesia and mechanical allodynia, but did not change thermal hyperalgesia. An obvious loss of all the sensitizations was observed after SNIs, SNIcp, and SNT, which were recognized as hypoalgesia. Related pain hypersensitivity was in correspondence with previous results in the variants of SNI, suggesting that mechanical hyperalgesia and mechanical allodynia are the main behavioral characters.

## *Cutaneous innervations following the Variants of SNI*

The skin territories in the foot sole supplied by each of the individual branch of the sciatic and femoral nerve have been distinctively identified in rats and mice.[3,8,42] Here, we focused on the first footpad, mainly a tibial skin territory, to investigate the possible changes of cutaneous innervation after the variants of SNI and SNT.

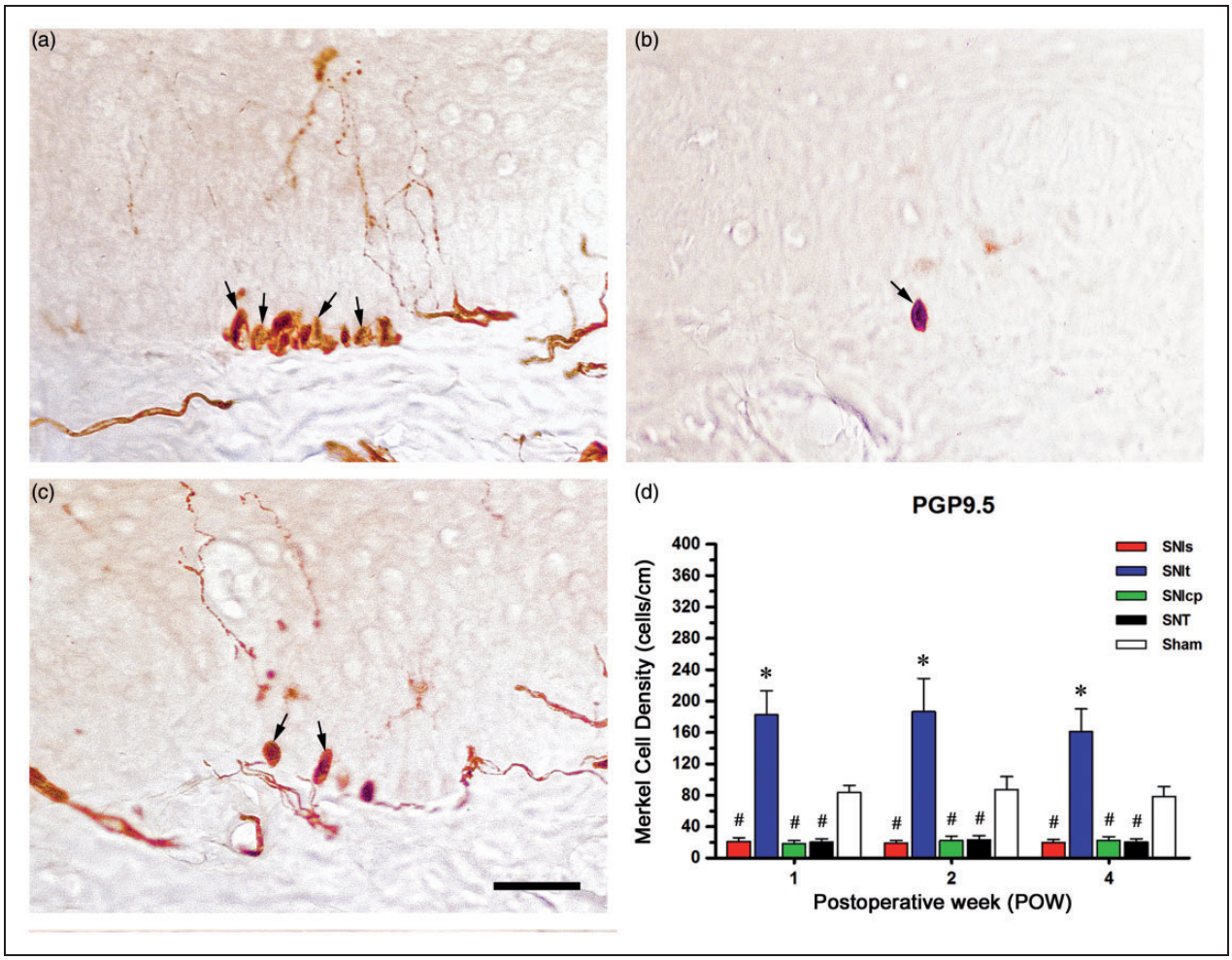


**Figure 7.** Clusters of Merkel cell in the stratum basale of the epidermis following SNIt. At POW1 after (a) SNIt, (b) SNIs, SNIcp, SNT, and (c) Sham, the footpad sections were immunostained with an antiserum against PGP9.5. (d) Merkel cell distributions were quantified by the temporal changes of morphological patterns in PGP9.5, which were represented as Merkel Cell Density (mean ± SD; $n = 5$ at each POW after the variants of SNI and Sham). Student's $t$ test was applied to examine the differences against Sham at each time point. * $p < 0.05$ indicated a significant difference versus Sham and # $p < 0.05$ indicated a significant difference versus Sham. Two-way repeated measures ANOVA was also performed following the Bonferroni's post hoc test. Scale bar = 50 μm.

Epidermal innervation showed that PGP9.5-IR IENFs in SNIt was similar to that in Sham rather than a complete loss of PGP9.5-IR IENFs in other SNI and SNT. Additionally, GAP43-IR IENFs presented as a comparable IENFs density between SNIt and Sham, which means there was no intact nerve terminal sprouting in the epidermis. Despite our previous results show that the increases of GAP43-IR IENFs after nerve decompression in CCI which represent as an enhancement of IENFs regeneration.[12] In recent times, intact CGRP-IR IENFs after SNI has been found to lead to epidermal reinnervation and hyperinnervation by collateral sprouting.[42] To look more deeply into this issue, our unpublished data excluded the possibility of collateral sprouting from the results of CGRP-IR IENFs after SNIs and SNT in the first footpad. We therefore recommended that normal epidermal innervation in the first footpad represents as a major morphological evidence for SNIt.

In CCI, we have previously shown a partial loss of CGRP- and NF200-IR SENFs and an increase of metabotropic glutamate receptor subtype 5-IR SENFs, which are supposed to be an outcome of nerve demyelination.[14] In this study, we found that PGP9.5- or GAP43-IR expressions observed in SENFs after SNIt were comparable to those after Sham. At the same time, there was not any significant difference between SNIt and Sham in NF200-IR SENFs, and it indicated that no changes were observed in myelinated A fibers. As a result, Taken together we concluded that a supportive morphological evidence in nerve terminal sprouting of the dermis after SNIt was in lack. Considering NF200-IR SENFs in SNI, an analogous result has been reported that nerve

terminal sprouting does not change in the sural skin territory.[42] Nevertheless, a complete loss of NF200-IR SENFs in tibial skin territory is noticeably inverted to a normal distribution at 10 weeks.[42]

### *Effects of PKCγ on mechanical hypersensitivity after SNIt*

In the dorsal horn, the binding of BDNF to TrkB receptor results in increasing the ability of phosphoinositide 3-kinase and pyruvate dehydrogenase kinase 1 (PDK1) for the regulation of neuronal plasticity.[18,43] One of PDK1 cascades is to control the activation of PKMζ, an atypical PKC isoform, which mediates in mechanical allodynia via the trafficking of the α-amino-3-hydroxy-5-methyl-4-isoxazolepropionic acid (AMPA) receptors.[18,32,44] Moreover, thermal hyperalgesia is induced by the activation of PKC delta (PKCδ), a novel PKC isoform, leading to the trafficking of NMDA receptors after the intraplantar injection of Bradykinin.[45] After CCI, the phosphorylation of AMPA and NMDA receptors is known to induce thermal hyperalgesia and mechanical allodynia by an increased PKCγ activity.[46,47] GF 109203X therefore is commonly used to attenuate mechanical hyperalgesia and mechanical allodynia by intrathecal injection in neuropathic pain models.[20,22,48] Here, we demonstrated that the increases of phospho-PKCγ expression in SENFs after SNIt were linked to mechanical hypersensitivity which was confirmed by the results of the intraplantar injection of GF 109203X. This is comparable to an earlier outcome that bisindolylmaleimide I, a PKC inhibitor, efficiently attenuates bradykinin-induced mechanical allodynia by intraplantar injection.[40] Additionally, the withdrawal thresholds in mechanical allodynia following SNI are increased in PKCγ knockout mice, whereas the conflicting results are observed in PKC alpha (PKCα) knockout mice.[23,24]

### *Role of mTOR in mechanical hypersensitivity following SNIt*

Based on the activation of TrkB receptor, another PDK1 cascade is to activate protein kinase B (Akt) for promoting mTOR to form mTOR complex 1, which modulates 4E-BP1 and S6K1 activities, thereby resulting in an increase of PKC lambda (PKCλ) and PKMζ.[25,32,49] mTOR therefore is known to be an important kinase for local protein synthesis in regulating neuronal plasticity.[26,49] mTOR complex 1 and its downstream effectors contribute to thermal hyperalgesia and mechanical allodynia in inflammatory pain models.[28,31,50] Several studies in SNI showed that the myelinated A fibers of the spinal rootlets and dermis increase mTOR, 4E-BP1, and S6K1 activities.[29,30,51] mTOR complex 1 inhibitors such as rapamycin and temsirolimus efficiently attenuate SNI-induced mechanical hyperalgesia and mechanical allodynia by intrathecal injections.[29] Additionally, mechanical allodynia and cold allodynia after SNI are reversed by intraplantar and intraperitoneal injections of temsirolimus and Torin 1 in mice.[51,52] In the present study, we found a persistent increase of phospho-mTOR-IR SENFs and emphasized the dose-dependent effects of rapamycin on mechanical hyperalgesia and mechanical allodynia by intraplantar injections following SNIt. However, it needs to know that unmyelinated C fibers are considered as another new target of rapamycin being demonstrated via electrophysiological recordings.[30]

### *Clusters of Merkel cell in the epidermis after SNIt*

Meissner's corpuscle, Merkel disk, Pacinian corpuscle, and Ruffini ending formed from myelinated Aβ fibers in the dermis of the skin are named as mechanoreceptors. Merkel disk mainly synapses together with a closely associated Merkel cell for transducing the senses of light and discriminative touch.[39,53] Here, we observed an increase of PGP9.5-IR Merkel cell clustered near the epidermal–dermal junction after SNIt. We therefore assumed that these Merkel cells might release some causal factors to induce the activation of PKCγ or mTOR in intact SENFs for mechanical hypersensitivity. Merkel cell reacted to histamine or activated transient receptor potential ion channel releases vasoactive intestinal peptide, which is in support of mechanotransduction in skin disorders.[54] Recently, a mechanically activated cation channel, Piezo2, increased in Merkel cell has been considered as a critical component of mechanical allodynia.[55,56]

## Conclusion

Our current findings in the rats after SNIt (spared tibial branch) indicate that (1) mechanical hyperalgesia and mechanical allodynia are significant developed; (2) cutaneous innervations according to the results of IENFs density and SENFs area are completely preserved in the first footpad; (3) the intense increases of phospho-PKCγ- and phospho-mTOR-IR expressions in intact SENFs are observed; and (4) mechanical hyperalgesia and mechanical allodynia are attenuated in a dose-dependent manner by the intraplantar injections of GF 109203X or rapamycin. Clusters of PGP9.5-IR Merkel cell might implied the formation of Merkel cell-neurite complexes played a part in inducing mechanotransduction. Overall, we strongly recommend that PKCγ activation and mTOR-dependent PKCγ synthesis in intact primary afferents appeared to be an essential target of therapeutic strategy for mechanical hypersensitivity following SNI.

## Authors' contributions

MHK performed most of the experiments and contributed to the analysis of the data. MLY performed the parts of drug administration and contributed to the analysis of the data. SCY was responsible for tissue processing and prepared the figures. CTL contributed to the planning of all experiments and wrote the manuscript. TJT was responsible for the coordination and overall supervision of the study, and edited the manuscript. All authors read and approved the final manuscript.

## Declaration of Conflicting Interests

The author(s) declared no potential conflicts of interest with respect to the research, authorship, and/or publication of this article.

## Funding

The author(s) disclosed receipt of the following financial support for the research, authorship, and/or publication of this article: This work was supported by the National Science Council (NSC 102-2320-B-040-024, NSC 104-2320-B-040-012) and Chung Shan Medical University (CSMU G102N0003), Taiwan. The funders had no role in study design, data collection and analysis, decision to publish, or preparation of the manuscript.

## References

1. Bennett GJ and Xie YK. A peripheral mononeuropathy in rat that produces disorders of pain sensation like those seen in man. *Pain* 1988; 33: 87–107.
2. Seltzer Z, Dubner R and Shir Y. A novel behavioral model of neuropathic pain disorders produced in rats by partial sciatic nerve injury. *Pain* 1990; 43: 205–218.
3. Decosterd I and Woolf CJ. Spared nerve injury: an animal model of persistent peripheral neuropathic pain. *Pain* 2000; 87: 149–158.
4. Abe K, Fujii Y and Nojima H. Evaluation of hyperalgesia in spared nerve injury model using mechanical, thermal, and chemical stimuli in the mouse. *Neurol Res* 2011; 33: 656–662.
5. Bourquin AF, Suveges M, Pertin M, et al. Assessment and analysis of mechanical allodynia-like behavior induced by spared nerve injury (SNI) in the mouse. *Pain* 2006; 122: 14.e1–14.
6. Smith AK, O'Hara CL and Stucky CL. Mechanical sensitization of cutaneous sensory fibers in the spared nerve injury mouse model. *Mol Pain* 2013; 9: 61.
7. Duraku LS, Hossaini M, Hoendervangers S, et al. Spatiotemporal dynamics of re-innervation and hyperinnervation patterns by uninjured CGRP fibers in the rat foot sole epidermis after nerve injury. *Mol Pain* 2012; 8: 61.
8. Duraku LS, Hossaini M, Schüttenhelm BN, et al. Re-innervation patterns by peptidergic Substance-P, non-peptidergic P2X3, and myelinated NF-200 nerve fibers in epidermis and dermis of rats with neuropathic pain. *Exp Neurol* 2013; 241: 13–24.
9. Kennedy WR. Opportunities afforded by the study of unmyelinated nerves in skin and other organs. *Muscle Nerve* 2004; 29: 756–767.
10. Tseng TJ, Chen CC, Hsieh YL, et al. Effects of decompression on neuropathic pain behaviors and skin reinnervation in chronic constriction injury. *Exp Neurol* 2007; 204: 574–582.
11. Ko MH, Hu ME, Hsieh YL, et al. Peptidergic intraepidermal nerve fibers in the skin contribute to the neuropathic pain in paclitaxel-induced peripheral neuropathy. *Neuropeptides* 2014; 48: 109–117.
12. Tseng TJ, Hsieh YL, Ko MH, et al. Redistribution of voltage-gated sodium channels after nerve decompression contributes to relieve neuropathic pain in chronic constriction injury. *Brain Res* 2014; 1589C: 15–25.
13. Lawson SN and Waddell PJ. Soma neurofilament immunoreactivity is related to cell size and fibre conduction velocity in rat primary sensory neurons. *J Physiol* 1991; 435: 41–63.
14. Ko MH, Hsieh YL, Hsieh ST, et al. Nerve demyelination increases metabotropic glutamate receptor subtype 5 expression in peripheral painful mononeuropathy. *Int J Mol Sci* 2015; 16: 4642–4665.
15. Xie HY, Xu F, Li Y, et al. Increases in PKC gamma expression in trigeminal spinal nucleus is associated with orofacial thermal hyperalgesia in streptozotocin-induced diabetic mice. *J Chem Neuroanat* 2015; 63: 13–19.
16. Hughes AS, Averill S, King VR, et al. Neurochemical characterization of neuronal populations expressing protein kinase C gamma isoform in the spinal cord and gracile nucleus of the rat. *Neuroscience* 2008; 153: 507–517.
17. Sandkuhler J. Understanding LTP in pain pathways. *Mol Pain* 2007; 3: 9.
18. Price TJ and Inyang KE. Commonalities between pain and memory mechanisms and their meaning for understanding chronic pain. *Prog Mol Biol Transl Sci* 2015; 131: 409–434.
19. Ruscheweyh R, Wilder-Smith O, Drdla R, et al. Long-term potentiation in spinal nociceptive pathways as a novel target for pain therapy. *Mol Pain* 2011; 7: 20.
20. Aira Z, Buesa I, García del Caño G, et al. Transient, 5-HT2B receptor-mediated facilitation in neuropathic pain: up-regulation of PKCγ and engagement of the NMDA receptor in dorsal horn neurons. *Pain* 2013; 154: 1865–1877.
21. Zhou XL, Zhang CJ, Wang Y, et al. EphrinB-EphB signaling regulates spinal pain processing via PKCγ. *Neuroscience* 2015; 307: 64–72.
22. Neumann S, Braz JM, Skinner K, et al. Innocuous, not noxious, input activates PKCγ interneurons of the spinal dorsal horn via myelinated afferent fibers. *J Neurosci* 2008; 28: 7936–7944.
23. Malmberg AB, Chen C, Tonegawa S, et al. Preserved acute pain and reduced neuropathic pain in mice lacking PKCγ. *Science* 1997; 278: 279–283.
24. Zhao C, Leitges M and Gereau RW 4th. Isozyme-specific effects of protein kinase C in pain modulation. *Anesthesiology* 2011; 115: 1261–1270.
25. Hay N and Sonenberg N. Upstream and downstream of mTOR. *Genes Dev* 2004; 18: 1926–1945.

26. Ma XM and Blenis J. Molecular mechanisms of mTOR-mediated translational control. *Nat Rev Mol Cell Biol* 2009; 10: 307–318.
27. Asante CO, Wallace VC and Dickenson AH. Mammalian target of rapamycin signaling in the spinal cord is required for neuronal plasticity and behavioral hypersensitivity associated with neuropathy in the rat. *J Pain* 2010; 11: 1356–1367.
28. Géranton SM, Jiménez-Díaz L, Torsney C, et al. A rapamycin-sensitive signaling pathway is essential for the full expression of persistent pain states. *J Neuroscience* 2009; 29: 15017–15027.
29. Liang L, Tao B, Fan L, et al. mTOR and its downstream pathway are activated in the dorsal root ganglion and spinal cord after peripheral inflammation, but not after nerve injury. *Brain Res* 2013; 1513: 17–25.
30. Jiménez-Díaz L, Géranton SM, Passmore GM, et al. Local translation in primary afferent fibers regulates nociception. *PLoS One* 2008; 3: e1961.
31. Xu Q, Fitzsimmons B, Steinauer J, et al. Spinal phosphinositide 3-kinase-Akt-mammalian target of rapamycin signaling cascades in inflammation-induced hyperalgesia. *J Neurosci* 2011; 31: 2113–2124.
32. Melemedjian OK, Tillu DV, Asiedu MN, et al. BDNF regulates atypical PKC at spinal synapses to initiate and maintain a centralized chronic pain state. *Mol Pain* 2013b; 9: 12.
33. Price TJ and Ghosh S. ZIPping to pain relief: the role (or not) of PKMζ in chronic pain. *Mol Pain* 2013; 9: 6.
34. IASP Committee. Ethical standards for investigations of experimental pain in animals. The Committee for Research and Ethical Issues of the International Association for the Study of Pain. *Pain* 1980; 9: 141–143.
35. Zimmermann M. Ethical guidelines for investigations of experimental pain in conscious animals. *Pain* 1983; 16: 109–110.
36. Wall PD, Devor M, Inbal R, et al. Autotomy following peripheral nerve lesions: experimental anaesthesia dolorosa. *Pain* 1979; 7: 103–111.
37. Intondi AB, Zadina JE, Zhang X, et al. Topography and time course of changes in spinal neuropeptide Y immunoreactivity after spared nerve injury. *Neuroscience* 2010; 165: 914–922.
38. Tal M and Bennett GJ. Extra-territorial pain in rats with a peripheral mononeuropathy: mechano-hyperalgesia and mechano-allodynia in the territory of an uninjured nerve. *Pain* 1994; 57: 375–382.
39. Christianson JA, Ryals JM, Johnson MS, et al. Neurotrophic modulation of myelinated cutaneous innervation and mechanical sensory loss in diabetic mice. *Neuroscience* 2007; 145: 303–313.
40. Souza AL, Moreira FA, Almeida KR, et al. In vivo evidence for a role of protein kinase C in peripheral nociceptive processing. *Br J Pharmacol* 2002; 135: 239–247.
41. Sakurada T, Mizoguchi H, Kuwahata H, et al. Intraplantar injection of bergamot essential oil induces peripheral antinociception mediated by opioid mechanism. *Pharmacol Biochem Behav* 2011; 97: 436–443.
42. Duraku LS, Hossaini M, Hoendervangers S, et al. Spatiotemporal dynamics of re-innervation and hyperinnervation patterns by uninjured CGRP fibers in the rat foot sole epidermis after nerve injury. *Mol Pain* 2012; 8: 61.
43. Vanelderen P, Rouwette T, Kozicz T, et al. The role of brain-derived neurotrophic factor in different animal models of neuropathic pain. *Eur J Pain* 2010; 14: 473.e1–9.
44. Wang Y, Wu J, Wu Z, et al. Regulation of AMPA receptors in spinal nociception. *Mol Pain* 2010; 6: 5.
45. Brenner GJ, Ji RR, Shaffer S, et al. Peripheral noxious stimulation induces phosphorylation of the NMDA receptor NR1 subunit at the PKC-dependent site, serine-896, in spinal cord dorsal horn neurons. *Eur J Neurosci* 2004; 20: 375–384.
46. Miletic G, Hermes JL, Bosscher GL, et al. Protein kinase C gamma-mediated phosphorylation of GluA1 in the postsynaptic density of spinal dorsal horn neurons accompanies neuropathic pain, and dephosphorylation by calcineurin is associated with prolonged analgesia. *Pain* 2015; 156: 2514–2520.
47. Mao J, Price DD, Phillips LL, et al. Increases in protein kinase C gamma immunoreactivity in the spinal cord dorsal horn of rats with painful mononeuropathy. *Neurosci Lett* 1995; 198: 75–78.
48. Velázquez KT, Mohammad H and Sweitzer SM. Protein kinase C in pain: involvement of multiple isoforms. *Pharmacol Res* 2007; 55: 578–589.
49. Leal G, Comprido D and Duarte CB. BDNF-induced local protein synthesis and synaptic plasticity. *Neuropharmacology* 2014; 76(Pt C): 639–656.
50. Norsted Gregory E, Codeluppi S, Gregory JA, et al. Mammalian target of rapamycin in spinal cord neurons mediates hypersensitivity induced by peripheral inflammation. *Neuroscience* 2010; 169: 1392–1402.
51. Obara I and Hunt SP. Axonal protein synthesis and the regulation of primary afferent function. *Dev Neurobiol* 2014; 74: 269–278.
52. Obara I, Géranton SM and Hunt SP. Axonal protein synthesis: a potential target for pain relief? *Curr Opin Pharmacol* 2012; 12: 42–48.
53. Lewin GR and Moshourab R. Mechanosensation and pain. *J Neurobiol* 2004; 61: 30–44.
54. Boulais N, Pereira U, Lebonvallet N, et al. Merkel cells as putative regulatory cells in skin disorders: an in vitro study. *PLoS One* 2009; 4: e6528.
55. Ikeda R, Cha M, Ling J, et al. Merkel cells transduce and encode tactile stimuli to drive Aβ-afferent impulses. *Cell* 2014; 157: 664–675.
56. Woo SH, Ranade S, Weyer AD, et al. Piezo2 is required for Merkel-cell mechanotransduction. *Nature* 2014; 509: 622–626.